ORIGINAL ARTICLE

Prediction model of machining surface roughness for five-axis machine tool based on machine-tool structure performance

Tzu-Chi Chan[1] · Hsin-Hsien Lin[1] · Sabbella Veera Venkata Satyanarayana Reddy[1]

Abstract

In this study, structural performance analysis and test verification of a machine tool were performed. This research is based on a five-axis machine tool for modeling and experimental verification. The mechanical-structure performance of the machine-tool cutting process directly affects the processing results. The processing performance of a five-axis machine tool was analyzed to identify processing weaknesses as the basis for subsequent structural improvements. Data were then integrated through the abductory induction mechanism (AIM) polynomial neural network to predict intelligent processing quality, and an in-depth investigation was conducted by importing processing parameters to predict the surface quality of the finished product. The finite-element analysis method was used to analyze the static and dynamic characteristics of the whole machine and to test the structural modal frequency and vibration shape. For modal testing, the experiment used various equipment, including impact hammers, accelerometers, and signal extractors. Subsequent planning of modal frequency band processing experiments was conducted to verify the influence of natural frequencies on the processing level. Finally, according to the machine processing characteristics, a processing experiment was planned. The measurement record was used as the training data of the AIM polynomial neural network to establish the processing quality prediction model. After analysis and an actual machine test comparison, the two-axis static rigidity values of the machine were X: 1.63 kg/μm and Y: 1.93 kg/μm. The modal vibration shape maximum error of the machine was within 6.2%. The processing quality prediction model established by the AIM polynomial neural network could input processing parameters to achieve the surface roughness prediction value, and the actual relative error of the Ra value was within 0.1 μm. Based on the results of cutting experiments, the influence of the dynamic characteristics of the machine on the processing quality was obtained, especially in the modal vibration environment, which had an adverse effect on the surface roughness. Hence, the surface roughness of the workpiece processed by the machine could be predicted.

Keywords Five-axis machine tool · Finite element method · Static stiffness · Modal analysis · Modal test · Abductory induction mechanism

Abbreviations
CPM Complexity penalty factor
FSE Fitting squared error
KP   Complexity penalty
PSE Predicted squared error

1 Introduction

A machine tool must have sufficient rigidity and optimized design considerations in the structural analysis stage to facilitate the best performance of the machine and to develop intelligent processing functions based on excellent machine performance. Therefore, many studies have been conducted in this area. Eynian [1] used mathematical models to determine the processing parameters that are required for stable, high-performance, and high-speed processing. These mathematical models must accurately measure the modal parameters of the processing system. Tang et al. [2] proposed a nonlinear tool mark coefficient recognition method using finite amplitude. The results showed that the size distribution of the critical depth of the cut is affected by the process damping, and the percentage increase in the cut depth is closely related to the tool direction and the frequency response function (FRF). Liu et al. [3] considered the effect of elastic interaction to analyze the influence of the anchor bolt pre-tightening sequence on the pre-tightening state. The results showed that the pre-tightening sequence from the

✉ Tzu-Chi Chan
  tcchan@nfu.edu.tw

1 Department of Mechanical and Computer-Aided
   Engineering, National Formosa University, Yunlin, Taiwan

middle to the side can ensure uniform deformation of the machine bed.

Muñoz-Escalona and Maropoulosb [4] studied a geometric model for predicting the surface roughness of square inserts in face milling. The Taguchi method was used as an experimental design, and the surface roughness of the milled surface was measured using a non-contact profiler. Zhao et al. [5] proposed a surface-roughness prediction model and showed that the tool posture has a significant influence on the surface roughness, which means that the angle of the tool can be controlled to improve the surface roughness of the processing. Wang et al. [6] proposed a five-axis tooth surface milling surface roughness control method using feed rate optimization based on surface topography analysis. According to this model, the influence of tool runout and workpiece curvature on the surface profile was analyzed.

Wang et al. [7] proposed a model by which the predicted surface morphology was determined, and the factors affecting the development trend of roughness were analyzed. Tomov et al. [8] suggested the relationship between the parameter-prediction model and the surface-roughness formation process. Das et al. [9] explored artificial neural networks and predicted the cutting force and surface roughness generated during CNC milling. García-Plaza et al. [10] optimized surface-roughness monitoring by focusing on vibration signal analysis. Accordingly, the signal statistical measurements and frequency bands were correlated with surface roughness. Rasagopal et al. [11] studied the influence of processing parameters on the surface roughness and cutting force of mixed aluminum metal matrix composites. The results were optimized and analyzed using the Taguchi method. Mansour and Abdalla [12] developed a mathematical model of surface roughness based on the cutting speed, feed rate, and cutting axial depth. Abouelatta and Mádl [13] identified a correlation between surface roughness and cutting vibration during turning and derived a mathematical model of the predicted roughness parameters based on cutting parameters and machine tool vibration. Lin et al. [14] constructed a prediction model for surface roughness and cutting force. Once the machining parameters are given, the surface roughness and cutting force can be predicted through the network. Ostasevicius et al. [15] proposed a method to improve the surface roughness. The method is based on the excitation of a specific higher vibration mode of the turning tool, and it reduces the harmful vibrations in the machine tool and workpiece system by increasing the energy dissipation inside the tool material. Sahin and Motorcu [16] found that the feed rate is the main factor affecting the surface roughness, and good agreement between the predicted and experimental surface roughness was observed within a reasonable range. Öktem et al. [17] studied the best cutting conditions to achieve the smallest surface roughness in mold surface milling. Lalwani et al. [18] studied the influence of cutting parameters on the cutting force and surface roughness in finishing hard turning. Davim et al. [19] established a surface roughness prediction model using neural networks using cutting conditions, such as cutting speed, feed rate, and cutting depth, as influencing factors. Their analysis showed that the cutting speed and feed rate have a significant effect on reducing the surface roughness, while the depth of cut has the smallest effect. Liu et al. [20] proposed a model that can provide valuable information about the effects of cutting parameters on surface roughness. Diniz and Micaroni [21] studied the effect of changing the cutting speed, feed, and nose radius on the surface roughness of a workpiece with and without cutting fluid. Muthukrishnan and Davim [22] used the input parameters of the cutting depth, cutting speed, and feed, and the output parameter was the surface finish of the machined part. The surface finish of machining can be predicted under cutting conditions within the operating range. Rawangwong et al. [23] used tungsten carbide tools for the face milling of semi-solid metal AA7075. They used Taguchi's experimental method to determine the cutting speed, feed rate, and depth of cut to obtain more satisfactory surface roughness. Wang et al. [24] used an abductive network to construct a network model, and one output was surface roughness. Chen et al. [25] proposed an abductory induction mechanism (AIM) polynomial network with the material properties provided as input to generate a model that predicts the tool geometry.

The machine tool industry is gradually advancing in terms of intelligent machine tool manufacturing. Accordingly, this study recorded the measurement results of the cutting experiment under different dynamic characteristics and parameters of the machine in the cases of the respective processing parameters, construction methods, and cutting materials. It employed a similar neural network construction to be effective. It is expected that the model for predicting the surface quality of the finished product can reduce processing costs and can thus be used as a basis for follow-up control experiments. When the processing parameters are imported, the surface roughness can be predicted using the network.

2 Materials and methods

The experimental hardware equipment used in this research included a five-axis machine tool, LM load cell, German Mahr sensor probe, Millimar C1200 displacement display meter (LVDT), impact hammer (Kistler 9726A20000), accelerometer (Endevco Model 65–100), spectrum analyzer, SE-4000 non-contact surface roughness meter, and Olympus STM 6 high-precision tool microscope. The software included the finite-element analysis software ANSYS Workbench, spectrum analysis software Novian,

modal post-processing software MEscope, static stiffness acquisition and analysis software, and the AIM polynomial neural network. The main process was to set the material parameters and boundary conditions, test static rigidity and dynamic characteristics, and perform further processing tests. The material properties are listed in Table 1.

In the meshing process, the element type was set to "tetrahedron," and mesh sizes were selected on the basis of the machine parts. The mesh size was set to 50.0 mm for the spindle seat and column, 20.0 mm for the screw, and 40.0 mm for the rest of the machine. The total number of nodes and elements was 351,004 and 200,994, respectively.

The X- and Y-axes values of the static rigidity apply a force of 2940 N at the head end of the spindle and a reaction force of 2940 N at the end of the table the torque and bearing load are applied at the end of the table. During the modal analysis, the foot was fixed according to the actual placement of the machine. The experimental process is illustrated in Fig. 1.

3 Analysis and test

When the machine is processing, the relative movement of the spindle end to the work platform affects the surface quality and accuracy of the workpiece. Therefore, static-rigidity simulation analysis was conducted for the spindle relative to the work platform. According to the analysis results, the X-axis relative displacement was 182.7 µm, and the static rigidity value was 1.64 (kg/µm). The Y-axis relative displacement was 145.5 µm, and the static rigidity value was 2.06 (kg/µm. The X- and Y-axes values of the static rigidity obtained from the analysis were 1.64 (kg/µm) and 2.06 (kg/µm), respectively, as shown in Fig. 2.

In the static rigidity experiment, the force application point was 100 mm below the nose of the spindle. The rotary table was used as a benchmark to test the corresponding axial rigidity of the machine spindle, as shown in Fig. 3. According to the experimental results, the static rigidity

values of the spindle end corresponding to the X- and Y-axes, measured on the basis of the rotating table, were 1.63 (kg/µm) and 1.93 (kg/µm), respectively (Fig. 4).

On comparing the analysis results with the actual test, the X-axis static stiffness error value was 0.7%, and the Y-axis static stiffness error value was 6.9%. The natural frequency analysis of the five-axis machine tool structure and the boundary conditions was set according to the actual fixed condition of the machine. We compared the main modes that have a greater impact on the processing performance, and we observed their mode shapes, including the torsion of the spindle and the column, as well as the torsion mode of the rotating table.

When performing modal experiments, it is necessary to devise a reasonable layout plan for the object to be tested while simultaneously confirming whether the position of the hitting point interferes with the position of the signal picked up by the accelerometer. The natural frequency of the structure is then analyzed, and the analysis model is compared with the actual machine vibration mode. The data collected in the experiment are imported into MEscope software, curve fitting is performed, and the sum of the imaginary part of the FRF is determined to calculate the frequency and damping value of each mode and to view the trend of each mode.

The distribution points of the accelerometers and the trigger point of the conducted modal experiment are shown in Fig. 5. The main distribution points, such as column, spindle, and rotating table, are the positions that directly affect the machining performance of the machine.

After comparing the results of finite element analysis (FEA) with those of experimental modal analysis (EMA), the maximum error ratio was 6.2%, the minimum error ratio was 2%, and the average error ratio was 4.7%, as shown in Table 2. These findings verify that the geometric model and parameter settings, such as the material properties and boundary conditions, are aligned with the characteristics of the actual machine.

4 Cutting experiment

In the cutting experiment, we used ultra-fine tungsten steel and aluminum end mills; the cutting material was Al-6061, and the processing method was down-milling. Different axial and radial depths of the cut conditions were used to explore the surface roughness results. The cutting diagram and milling cutter specifications are shown in Fig. 6.

In this study, the processing parameters of UX300 machine were determined experimentally. The tools and cutting material were initially fixed, and the processing parameters were used as the software input variables. The input data were as follows: spindle speed (rpm), feed rate (F), axial

Table 1 Material properties

| Gray cast iron (FC300)	
Density (kg/m^3)	7300
Young's modulus (Pa)	1.15×10^{11}
Poisson's ratio	0.25
Thermal conductivity (W/m °C)	45
Stainless steel 304	
Density (kg/m^3)	7750
Young's modulus (Pa)	1.93×10^{11}
Poisson's ratio	0.31
Thermal conductivity (W/m °C)	16.3

Fig. 1 Research flow chart
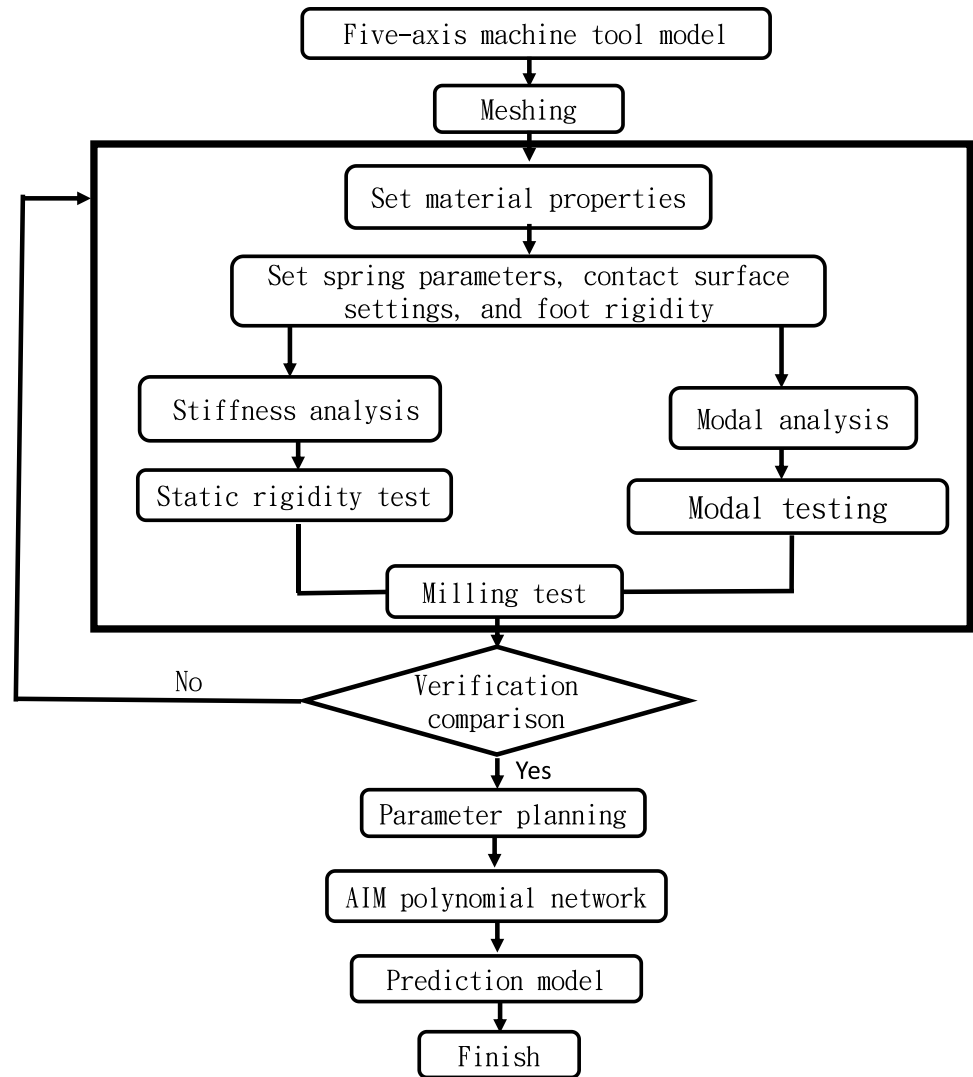
direction (ap), and radial depth of cut (ae), and the values of these parameters are listed in Table 3. The measurement results of the SE-4000 non-contact surface roughness

measuring instrument were set as the output data, which was the surface roughness, Ra, value of the workpiece. The processing methods and measurement parameters are shown
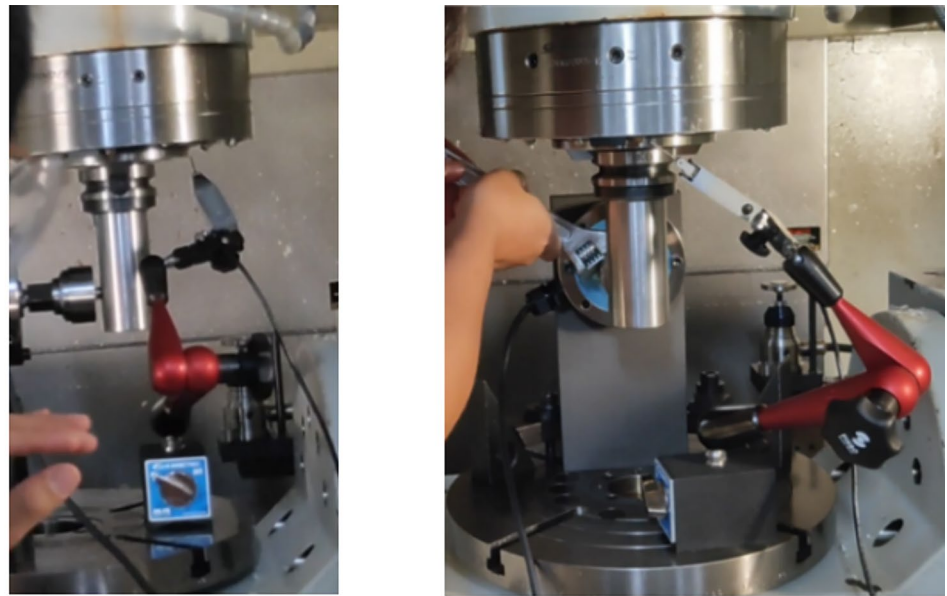
Fig. 2 Spindle vs. rotating worktable (*X*- and *Y*-axes values of the static rigidity were 1.64 (kg/μm) and 2.06 (kg/μm), respectively
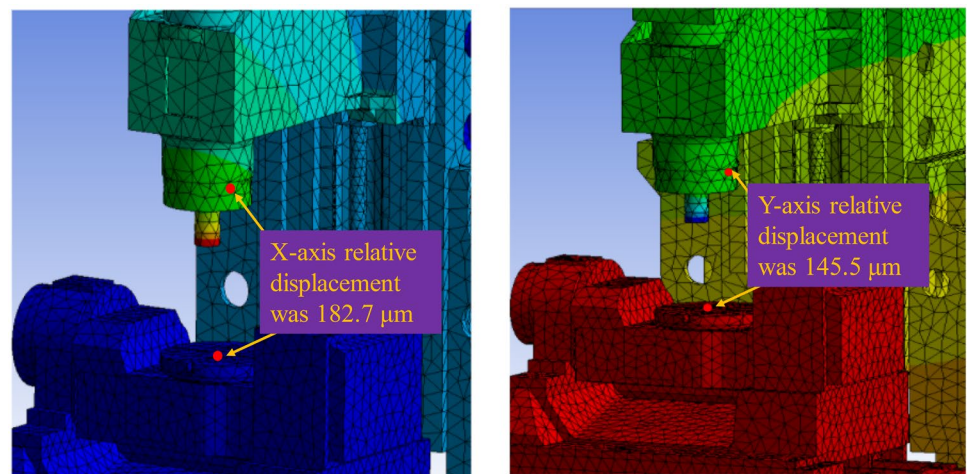
(a) Static rigidity analysis-X axis

(b) Static rigidity analysis-Y axis

X-axis relative displacement was 182.7 μm

Y-axis relative displacement was 145.5 μm

Fig. 3 Machine processing platform for determining the *X*- and *Y*-axes values of static rigidity


(a) X-axis static rigidity test **(b)** Y-axis static rigidity test

in Fig. 7. For modeling, the input and output factors were fit into a polynomial network model. The processing test data in the range of 4000–9000 rpm are listed in Tables 4, 5, 6, 7, 8 and 9, respectively.

Based on the modal analysis and the experimental results, a cutting experiment was conducted to assess the vibration shape trend of the entire machine, and the relative movement of the spindle end and the working platform was divided. First, the spindle speed was set to 4066 rpm (67.7 Hz) by

down milling. The main mode was the spindle vibration relative to the worktable. The surface roughness of each point was measured five times, approximately. The surface roughness obtained by processing was Ra 0.54 µm, as shown in Fig. 8a. The rotation speed was 5226 rpm (87.1 Hz) using the down milling method. The main mode was the spindle vibrating up and down relative to the worktable. The surface roughness obtained by machining was Ra 16.96 µm. The surface after cutting using the tool is shown in Fig. 8b.
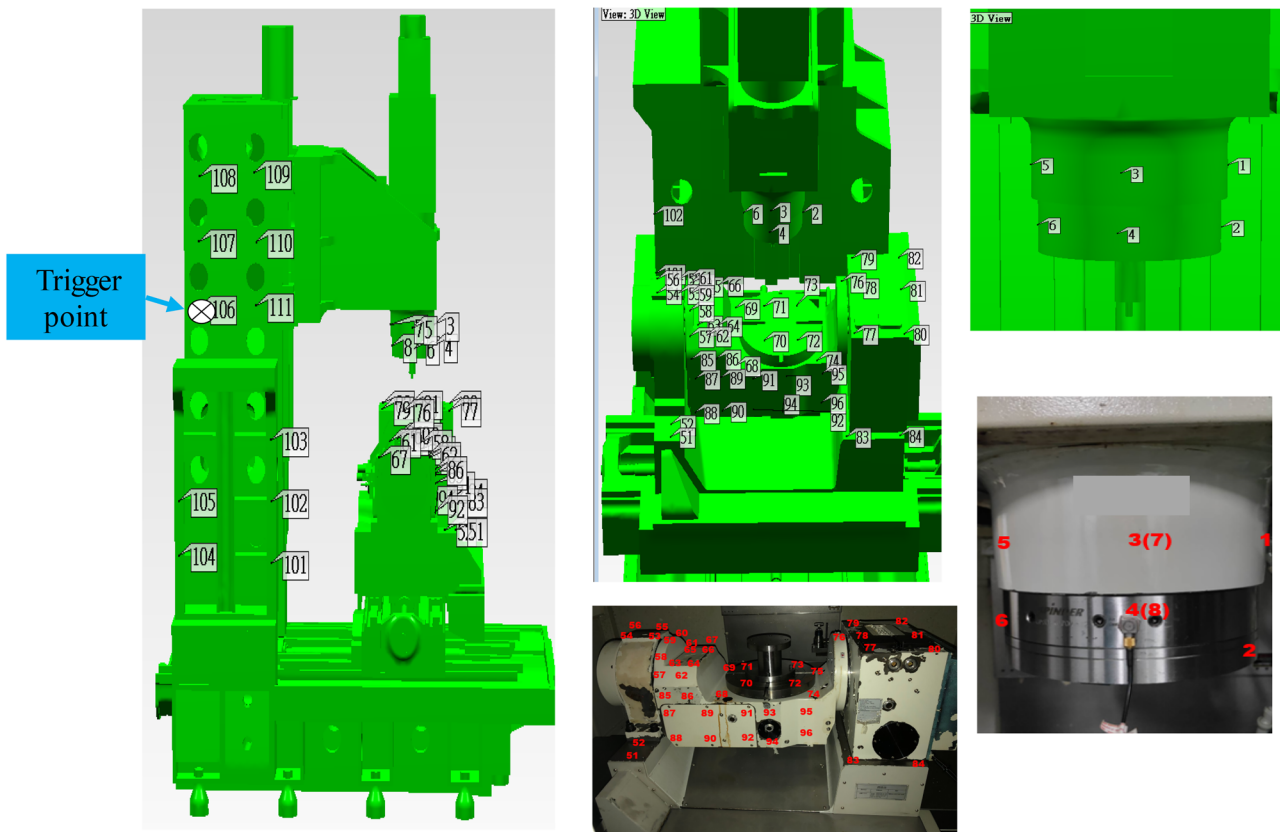
Fig. 4 Static rigidity data analysis
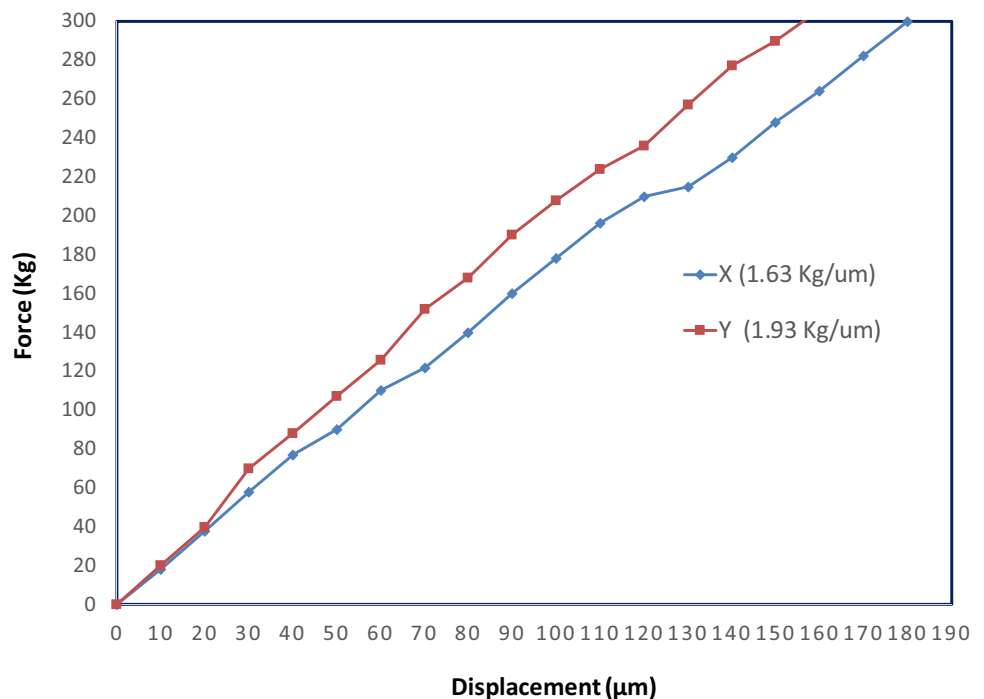
Fig. 5 The distribution points of the modal experiment

5 Prediction model and cutting testing

A polynomial network was employed to construct the predictive model, decompose the complex system into relatively simple subsystems through polynomial function nodes, and then combine the subsystems into many different levels. The input data were subdivided simultaneously and transmitted to each functional node. The function node used a polynomial function to calculate a limited amount of input data and obtain an output as the input of the next layer. Thus, the training structure of the entire polynomial network was established sequentially, as shown in Fig. 9. Subsequently, the optimal network construction, hierarchical features, and functional nodes were automatically generated according to the predicted square-error rule.

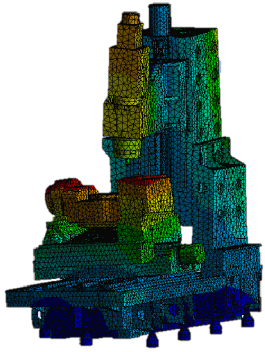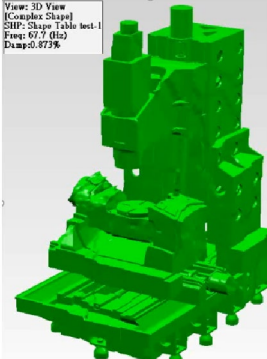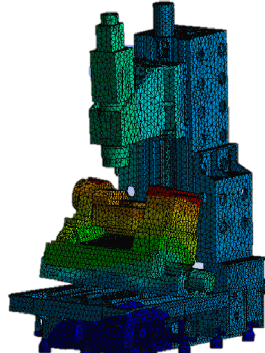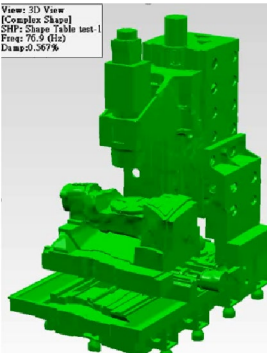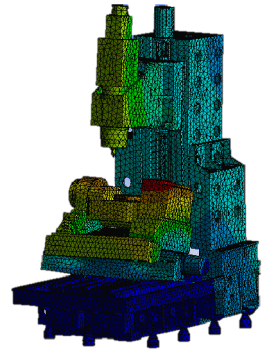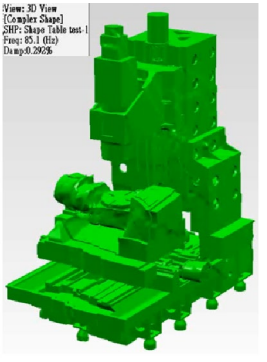The polynomial function reorganizes all polynomial node patterns as follows:

$$y_1 = w_0 + \sum_{i=1}^{m} W_i X_i + \sum_{i=1}^{m} \sum_{j=1}^{m} W_{ij} X_i X_j \\ + \sum_{i=1}^{m} \sum_{j=1}^{m} \sum_{k=1}^{m} W_{ijk} X_i X_j X_k + \cdots \cdots \tag{1}$$

where X_i, X_j and X_k are the input values, y_1 is the output value, and W_i, W_j and W_k are the coefficients of the polynomial function node. Commonly used polynomial nodes are the normalizer, single node, double node, triple node, white node, and unitizer. The definitions are as follows:

1. Normalizer: converts the original variable into a normalized input variable; the average is 0, the variance is 1, and its polynomial function is expressed as $y_1 = w_0 + w_i x_i$, where xi is the original input variable; y_1 is the normalized output variable; and w_0 and w_i are the coefficients.

2. Single node: refers to a single input variable The output and input variables have a third-order polynomial relationship. The polynomial function is expressed as $y_1 = w_0 + w_1 x_1 + w_2 x_1^2 + w_3 x_1^3$, where x_1 is an input variable, y_1 is an output variable, and w_0, w_1, w_2 and w_3 are coefficients.

3. Double node: the two input variables, the output variable, and the input variable have a third-order polynomial relationship. The polynomial function is expressed as $y_1 = w_0 + w_1 x_1 + w_2 x_2 + w_3 x_1^2 + w_4 x_2^2 + w_5 x_1 x_2 + w_6 x_1^3 + w_7 x_2^3$, where x_1, x_2 are input variables; y_1 is the output variable, and w_0, w_1, w_2,....w_7 are coefficients.

4. Triple node: refers to the three input variables. The output variable and the input variable have a third-order polyno-

Table 2 Comparison of natural frequency between model and actual machine

Content	Modal analysis	Modal testing	Feature
Mode shape			Spindle, column and rotary table swing horizontally back and forth
Frequency	69.1 Hz	67.7 Hz	2.1%
Mode shape			The main shaft and column swing up and down, and the rotary table swings back and forth
Frequency	72.1 Hz	76.9 Hz	6.2%
Mode shape			The main shaft and column swing up and down, and the rotary table swings back and forth
Frequency	90.0 Hz	85.1 Hz	5.8%

mial relationship, and the polynomial function is expressed as $y_1 = w_0 + w_1 x_1 + w_2 x_2 + w_3 x_3 + w_4 x_1{}^2 + w_5 x_2{}^2 + w_6 x_3{}^2 + w_7 x_1 x_2 + w_8 x_1 x_3 + w_9 x_2 x_3 + w_{10} x_1 x_2 x_3 + w_{11} x_1{}^3 + w_{12} x_2{}^3 + w_{13} x_3{}^3$, where x_1, x_2 and x_3 are input variables, y_1 is the output variable, and $w_0, w_1, w_2, \ldots\ldots w_{13}$ are coefficients.

5. White node: refers to n input variables, the output variable and the input variable are first-order polynomial relationships, and the polynomial function is expressed as $y_1 = w_0 + w_1 x_1 + w_2 x_2 + w_3 x_3 + \cdots + w_n x_n$, where x_1, $x_2, \ldots x_n$ are input variables, y_1 is an output variable, and $w_0, w_1, w_2, \ldots w_n$ are coefficients.

6. Unitizer: converts the output variable of the network into an actual output variable, and its polynomial function is expressed as $y_1 = w_0 + w_1 x_1$, where x_1 is the input variable, y_1 is the output variable, and w_0 and w_1 are coefficients.

The polynomial function node is used to construct the prediction model of the processing parameters and surface

Fig. 6 Cutting diagram and milling cutter specifications

Number of teeth	2
Helix angle (degrees)	40.0
Dc (mm)	6.0
Lc (mm)	16.0
L (mm)	50.0
d (mm)	6.0
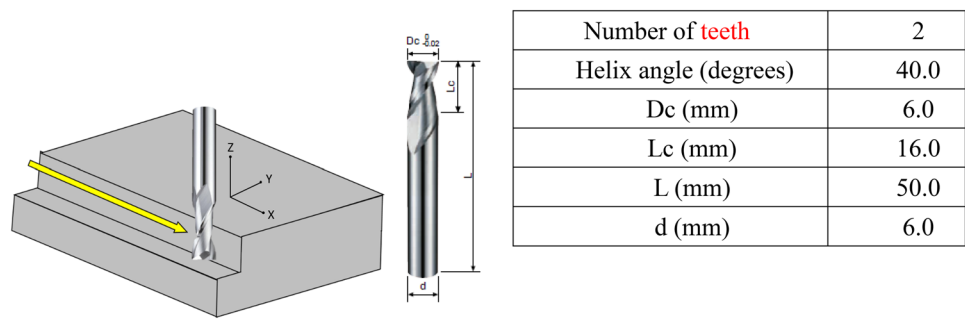
roughness Ra values. The polynomial network filters variables that have no contribution. The output of any node can be used as the input of the next layer and is combined with the original input for subsequent comparison. The network is synthesized layer by layer until the network mode converges and satisfies the prediction square error (PSE) rule.

Before constructing a polynomial network, it is necessary to import training data, learn the synthesis algorithm through the polynomial network, and determine the best network structure according to the minimum prediction square error method. PSE is a heuristic measurement of the expected square error of a network of independent data. PSE is defined as

$$PSE = FSE + KP \tag{2}$$

The fitting square error (FSE) occurs when constructing a network model with the training data. FSE can be expressed as

$$FSE = \frac{1}{n}\sum_{i=1}^{N}(\overline{y_i} - y_i)^2 \tag{3}$$

where n is the number of training data, $\overline{y_i}$ is the expected value of the training combination, and y_i is the predicted value obtained from the network. Additionally, KP is the complexity penalty, and its value can be obtained from Eq. (4):

$$KP = CPM \times \frac{2K}{N}\sigma p^2 \tag{4}$$

where K is the number of coefficients in the network, N is the number of training data, and σp^2 is the number of error variances between the prediction model and

Table 3 Cutting parameters

Material	Aluminum 6061-T6
Spindle speed	4000–9000 rpm
Feed per tooth	0.0375 mm/tooth, 0.08 mm/tooth
Feed rate	300–1440 mm/min
Cut deep	1 mm, 2 mm, 3 mm
Cut width	0.5, 1.0 mm

the actual model from the training database of the synthetic network. The complexity penalty factor (CPM) is an adjustable parameter that is used when synthesizing a polynomial network model. When N increases or σp^2 decreases, a polynomial network is used to construct the training data, which has higher credibility, and the network structure becomes more complex.

In Eq. (4), the matching accuracy increases as the PSE decreases. Under normal circumstances, the more complex the network model, the smaller the FSE value, and the higher the matching accuracy. In other words, the more complex the network, the greater is the KP value. Therefore, PSE produces a trade-off between network model complexity and accuracy. In the network synthesis and calculation, the best network refers to the network with the smallest PSE value. Moreover, the CPM can be used to adjust the balance between the model complexity and accuracy, as shown in Fig. 10. When the CPM value in the PSE increases, a more complex network is avoided. Conversely, when the CPM value decreases, a more complex network is adopted.

The reliability of the model was verified by predicting the parameters that had not been tested through the AIM polynomial network model. The results were then compared with those of the machine processing. The AIM software parameters were adjusted to a suitable fit and could then be converted into program codes and added to the machine controller. The input enables an AIM polynomial network model to adjust the parameters so that the FSE and PSE in the network model fit and converge to find an optimized network model. The adjustment parameters include the complexity penalty factor (CPM), number of layers, overfit penalty factor (overfit penalty), limiting factor (carving limit), and other parameters. Figure 11 shows the surface roughness polynomial model. The optimal model parameters were the complexity penalty factor (CPM) setting value of 0.01, number of layers, overfitting penalty factor of 1.0, and limit factor of 0.8. As shown in the Fig. 11, the nodes have several normalizers, triangles, a single double, and a single unitizer. The polynomial function nodes are as follows:

Fig. 7 Processing method and
measurement parameters
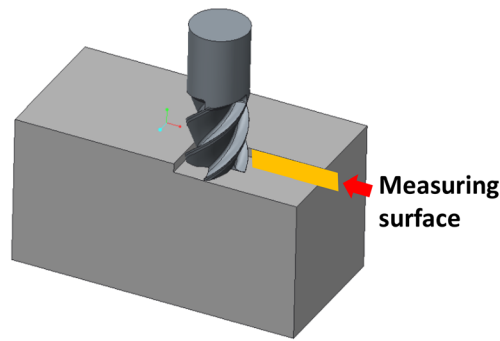
Measuring length range (section)	Cutoff x5
Measuring vertical range (magnification)	5000
Measurement level range (magnification)	50
Cutoff (mm)	0.8
Measuring speed (mm/s)	0.5

Table 4 Cutting training data for 4000 rpm

Spindle speed (rev/min)	Parameter		Cutting condition		Ra (μm)
	Feed rate (mm/min)	Feed per tooth (mm)	ap (mm)	ae (mm)	
4000	300	0.0375	1	0.5	0.48
4000	300	0.0375	1	1	0.44
4000	300	0.0375	2	0.5	0.46
4000	300	0.0375	2	1	0.45
4000	300	0.0375	3	0.5	0.44
4000	300	0.0375	3	1	0.49
4000	640	0.08	1	0.5	0.57
4000	640	0.08	1	1	0.53
4000	640	0.08	2	0.5	0.44
4000	640	0.08	2	1	0.42
4000	640	0.08	3	0.5	0.40
4000	640	0.08	3	1	0.45

Table 6 Cutting training data for 6000 rpm

Spindle speed (rev/min)	Parameter		Cutting condition		Ra (μm)
	Feed rate (mm/min)	Feed per tooth (mm)	ap (mm)	ae (mm)	
6000	450	0.0375	1	0.5	0.43
6000	450	0.0375	1	1	0.57
6000	450	0.0375	2	0.5	0.42
6000	450	0.0375	2	1	0.50
6000	450	0.0375	3	0.5	0.36
6000	450	0.0375	3	1	0.28
6000	960	0.08	1	0.5	0.61
6000	960	0.08	1	1	0.48
6000	960	0.08	2	0.5	0.45
6000	960	0.08	2	1	0.58
6000	960	0.08	3	0.5	0.36
6000	960	0.08	3	1	0.38

Table 5 Cutting training data for 5000 rpm

Spindle speed (rev/min)	Parameter		Cutting condition		Ra (μm)
	Feed rate (mm/min)	Feed per tooth (mm)	ap (mm)	ae (mm)	
5000	375	0.0375	1	0.5	0.39
5000	375	0.0375	1	1	0.52
5000	375	0.0375	2	0.5	0.41
5000	375	0.0375	2	1	0.47
5000	375	0.0375	3	0.5	0.32
5000	375	0.0375	3	1	0.38
5000	800	0.08	1	0.5	0.52
5000	800	0.08	1	1	0.64
5000	800	0.08	2	0.5	0.43
5000	800	0.08	2	1	0.55
5000	800	0.08	3	0.5	0.43
5000	800	0.08	3	1	0.41

Table 7 Cutting training data for 7000 rpm

Spindle speed (rev/min)	Parameter		Cutting condition		Ra (μm)
	Feed rate (mm/min)	Feed per tooth (mm)	ap (mm)	ae (mm)	
7000	525	0.0375	1	0.5	0.35
7000	525	0.0375	1	1	0.37
7000	525	0.0375	2	0.5	0.32
7000	525	0.0375	2	1	0.47
7000	525	0.0375	3	0.5	0.33
7000	525	0.0375	3	1	0.30
7000	1120	0.08	1	0.5	0.42
7000	1120	0.08	1	1	0.55
7000	1120	0.08	2	0.5	0.37
7000	1120	0.08	2	1	0.55
7000	1120	0.08	3	0.5	0.33
7000	1120	0.08	3	1	0.37

Table 8 Cutting training data for 8000 rpm

Spindle speed (rev/min)	Parameter		Cutting condition		Ra (µm)
	Feed rate (mm/min)	Feed per tooth (mm)	ap (mm)	ae (mm)	
8000	600	0.0375	1	0.5	0.38
8000	600	0.0375	1	1	0.40
8000	600	0.0375	2	0.5	0.40
8000	600	0.0375	2	1	0.42
8000	600	0.0375	3	0.5	0.27
8000	600	0.0375	3	1	0.26
8000	1280	0.08	1	0.5	0.39
8000	1280	0.08	1	1	0.46
8000	1280	0.08	2	0.5	0.37
8000	1280	0.08	2	1	0.46
8000	1280	0.08	3	0.5	0.34
8000	1280	0.08	3	1	0.36

Table 9 Cutting training data for 9000 rpm

Spindle speed (rev/min)	Parameter		Cutting condition		Ra (µm)
	Feed rate (mm/min)	Feed per tooth (mm)	ap (mm)	ae (mm)	
9000	675	0.0375	1	0.5	0.48
9000	675	0.0375	1	1	0.39
9000	675	0.0375	2	0.5	0.35
9000	675	0.0375	2	1	0.32
9000	675	0.0375	3	0.5	0.33
9000	675	0.0375	3	1	0.25
9000	1440	0.08	1	0.5	0.50
9000	1440	0.08	1	1	0.44
9000	1440	0.08	2	0.5	0.45
9000	1440	0.08	2	1	0.47
9000	1440	0.08	3	0.5	0.37
9000	1440	0.08	3	1	0.35

Fig. 8 **a** Spindle speed: 4066 rpm (67.7 Hz). The spindle end moves left and right relative to the table; **b** spindle speed: 5226 rpm (87.1 Hz). The spindle end moves up and down relative to the worktable
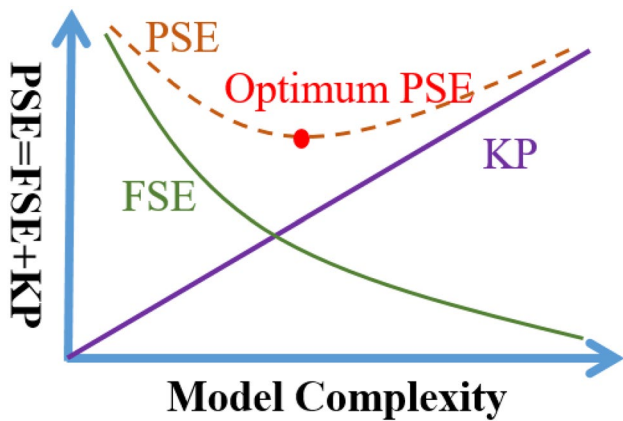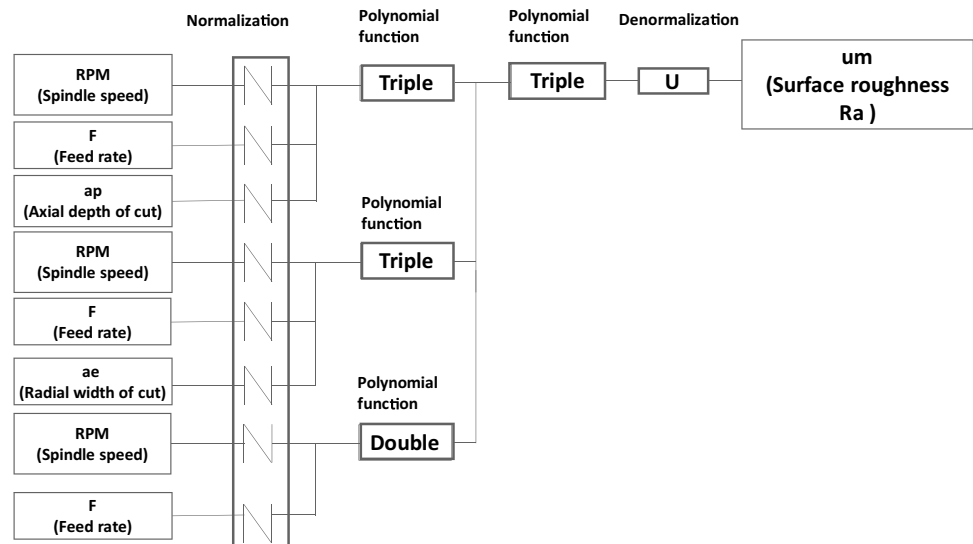
Ra 0.54 µm

(a)
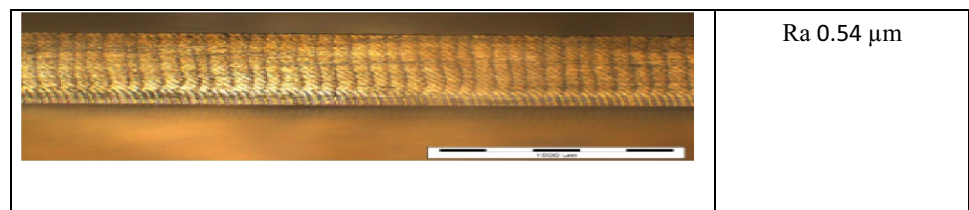
Ra 16.96 µm

(b)

Fig. 9 Synthetic polynomial network planning diagram

6 Prediction model and verification

By importing the machining parameter data that have not yet undergone cutting experiments into the AIM polynomial network model, the predicted surface roughness Ra value can be obtained, and the actual machining and predicted results can be compared. The surface roughness error range is approximately within the Ra value of 0.1 μm. The experimental findings show that the parameter processing results are within the predictable range; that is, this polynomial network model has a certain degree of reference value, and the quality of the processed surface can be predicted from the polynomial model, as shown in Table 10.
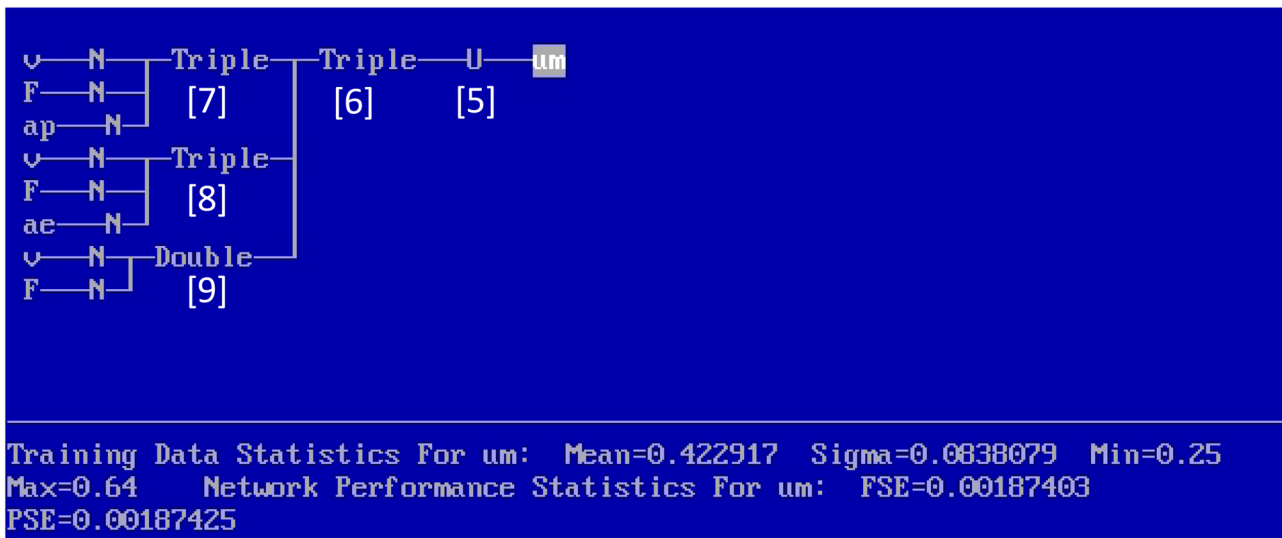

Fig. 10 Convergent prediction square error

Training Data Statistics For um: Mean=0.422917 Sigma=0.0838079 Min=0.25
Max=0.64 Network Performance Statistics For um: FSE=0.00187403
PSE=0.00187425

Fig. 11 AIM polynomial network

Table 10 Polynomial network model and results

Spindle speed (rev/min)	Parameter		Cutting condition		Ra (µm)	AIM predict Ra (µm)	Ra difference (µm)
	Feed rate (mm/ min)	Feed per tooth (mm)	ap (mm)	ae (mm)			
4000	320	0.04	1	0.75	0.45	0.45	0
4500	360	0.04	1	0.5	0.42	0.46	0.04
4500	360	0.04	0.5	1	0.45	0.52	0.07
5000	500	0.05	1	0.75	0.42	0.49	0.07
5000	500	0.05	1	0.5	0.40	0.48	0.08
5500	550	0.05	2	0.5	0.36	0.44	0.08
6000	720	0.06	2	0.75	0.36	0.45	0.09
6500	780	0.06	1.5	1	0.47	0.50	0.03
6500	780	0.06	2	0.5	0.40	0.40	0
7000	980	0.07	2	0.75	0.40	0.44	0.04
7500	1050	0.07	1.5	1	0.44	0.48	0.04
7500	1050	0.07	3	1	0.33	0.34	0.01
8000	1280	0.08	3	0.75	0.37	0.33	0.04
8500	1360	0.08	3	1	0.39	0.37	0.02
8500	1360	0.08	2.5	0.5	0.36	0.39	0.03
9000	1620	0.09	2	0.5	0.44	0.43	0.01
9500	1710	0.09	2.5	0.5	0.43	0.46	0.03
10,000	2000	0.10	0.5	0.5	0.43	0.44	0.01

7 Conclusion

The starting point of this study was the machine model analysis. A virtual machine model of the five-axis machine tool UX300 was constructed using ANSYS for static rigidity and dynamic analysis. The boundary conditions and material properties were improved by comparing the actual machine characteristics to simulate the real scenario. Static rigidity and modal experiments were performed to prove this finding of improvement. The static rigidity values of the two axes of the five-axis machine tool spindle against the bed were X: 1.63 kg/µm and Y: 1.93 kg/µm; the maximum modal error ratio was 6.2%, the minimum error ratio was 2%, and the average error ratio was 4.7%.

After studying and understanding the dynamic characteristics of the machine in depth, we planned the modal frequency band processing parameters and conducted modal cutting experiments to prove that the machine processing frequency had a substantial impact on the surface quality of the finished product. Subsequent planning of large data cutting experiments was used to develop intelligent processing by using the AIM polynomial neural network to train the surface roughness Ra value prediction model, constructing the correlation equation between cutting parameters, and determining the surface roughness model prediction results. The prediction error was within a certain range of the surface roughness Ra value of 0.1 µm.

Declarations

Conflicts of interest The authors declare no competing interests.

References

1. Eynian M (2019) In-process identification of modal parameters using dimensionless relationships in milling chatter. Int J Mach Tools Manuf 143:49–62
2. Tang X, Peng F, Yan R, Zhu Z, Li Z, Xin S (2021) Nonlinear process damping identification using finite amplitude stability and the influence analysis on five-axis milling stability. Int J Mech Sci 190:106008
3. Liu H, Wu J, Liu K, Kuang K, Luo Q, Liu Z, Wang Y (2019) Pretightening sequence planning of anchor bolts based on structure uniform deformation for large CNC machine tools. Int J Mach Tools Manuf 136:1–18
4. Muñoz-Escalonaa P, Maropoulosb PG (2015) A geometrical model for surface roughness prediction when face milling Al 7075–T7351 with square insert tools. J Manuf Syst 36:216–223
5. Zhao Z, Wang S, Wang Z, Liu N, Wang S, Ma C, Yang B (2020) Interference- and chatter-free cutter posture optimization towards

minimal surface roughness in five-axis machining. Int J Mech Sci 171:105395

6. Wang L, Ge S, Si H, Yuan X, Duan F (2020) Roughness control method for five-axis flank milling based on the analysis of surface topography. Int J Mech Sci 169:105337

7. Wang L, Ge S, Si H, Guan L, Duan F, Liu Y (2020) Elliptical model for surface topography prediction in five-axis flank milling. Chin J Aeronaut 33(4):1361–1374

8. Tomov M, Kuzinovski M, Cichosz P (2016) Development of mathematical models for surface roughness parameter prediction in turning depending on the process condition. Int J Mech Sci 113:120–132

9. Das B, Roy S, Rai RN, Saha SC (2016) Study on machinability of in situ Al–4.5%Cu–TiC metal matrix composite-surface finish, cutting force prediction using ANN. CIRP J Manuf Sci Technol 12:67–78

10. García-Plaza E, Núñez Lópeza PJ, Beamud Gonzálezb EM (2019) Efficiency of vibration signal feature extraction for surface finish monitoring in CNC machining. J Manuf Process 44:145–157

11. Rasagopal P, Senthilkumar P, Nallakumarasamy G, Magibalan S (2020) A study surface integrity of aluminum hybrid composites during milling peration. J Market Res 9(3):4884–4893

12. Mansour A, Abdalla H (2002) Surface roughness model for end milling: a semi-free cutting carbon casehardening steel (EN32) in dry condition. J Mater Process Technol 124:183–191

13. Abouelatta OB, Mádl J (2001) Surface roughness prediction based on cutting parameters and tool vibrations in turning operations. J Mater Process Technol 118(1–3):269–277

14. Lin WS, Lee BY, Wu CL (2001) Modeling the surface roughness and cutting force for turning. J Mater Process Technol 108:286–293

15. Ostasevicius V, Gaidys R, Rimkeviciene J, Dauksevicius R (2010) An approach based on tool mode control for surface roughness reduction in high-frequency vibration cutting. J Sound Vib 329:4866–4879

16. Sahin Y, Motorcu AR (2008) Surface roughness model in machining hardened steel with cubic boron nitride cutting tool. Int J Refract Metal Hard Mater 26:84–90

17. Öktem H, Erzurumlu T, Kurtaran H (2005) Application of response surface methodology in the optimization of cutting conditions for surface roughness. J Mater Process Technol 170:11–16

18. Lalwani DI, Mehta NK, Jain PK (2008) Experimental investigations of cutting parameters influence on cutting forces and surface roughness in finish hard turning of MDN250 steel. J Mater Process Technol 206:167–179

19. Davim JP, Gaitonde VN, Karnikc SR (2008) Investigations into the effect of cutting conditions on surface roughness in turning of free machining steel by ANN models. J Mater Process Technol 205:16–23

20. Liu N, Wang SB, Zhang YF, Lu WF (2016) A novel approach to predicting surface roughness based on specific cutting energy consumption when slot milling Al-7075. Int J Mech Sci 118:13–20

21. Diniz AE, Micaroni R (2002) Cutting conditions for finish turning process aiming: the use of dry. Int J Mach Tools Manuf 42:899904

22. Muthukrishnan N, Davim JP (2009) Optimization of machining parameters of Al/SiC-MMC with ANOVA and ANN analysis. J Mater Process Technol 209:225–232

23. Rawangwong S, Chatthong J, Boonchouytan W, Burapa R (2014) Influence of cutting parameters in face milling semi-solid AA7075 using carbide tool affected the surface roughness and tool wear. Energy Procedia 56:448–457

24. Wang YC, Chen CH, Lee BY (2009) The predictive model of surface roughness and searching system in database for cutting tool grinding. Mater Sci Forum 626–627:11–16

25. Chen J-Y, Chan T-C, Lee B-Y, Liang C-Y (2020) Prediction model of cutting edge for end mills based on mechanical material properties. Int J Adv Manuf Technol 107:2939–2951